

## NMR Study of the Mott Transitions to Superconductivity in the Two Cs<sub>3</sub>C<sub>60</sub> Phases

Y. Ihara,<sup>1,\*</sup> H. Alloul,<sup>1</sup> P. Wzietek,<sup>1</sup> D. Pontiroli,<sup>2</sup> M. Mazzani,<sup>2</sup> and M. Riccò<sup>2</sup>

<sup>1</sup>*Laboratoire de Physique des Solides, Université Paris-Sud 11, CNRS UMR 8502, 91405 Orsay, France*

<sup>2</sup>*Dipartimento di Fisica, Università di Parma, Via G. P. Usberti 7/a, 43100 Parma, Italy*

(Received 18 March 2010; published 23 June 2010)

We report a NMR and magnetometry study on the expanded intercalated fulleride Cs<sub>3</sub>C<sub>60</sub> in both its A15 and face centered cubic structures. NMR allowed us to evidence that both exhibit a first-order Mott transition to a superconducting state, occurring at distinct critical pressures  $p_c$  and temperatures  $T_c$ . Though the ground state magnetism of the Mott phases differs, their high  $T$  paramagnetic and superconducting properties are found similar, and the phase diagrams versus unit volume per C<sub>60</sub> are superimposed. Thus, as expected for a strongly correlated system, the interball distance is the relevant parameter driving the electronic behavior and quantum transitions of these systems.

DOI: 10.1103/PhysRevLett.104.256402

PACS numbers: 71.30.+h, 74.25.nj, 74.70.Wz

Superconductivity (SC) in the vicinity of magnetic phases is rather commonly found nowadays, especially in materials involving transition metal ions. There, the incidence of the spin fluctuations on the SC state and the symmetry of its order parameter are being highly debated and various possibilities have been considered depending on whether the electronic states involved at the Fermi level reside on a single orbital (as in the cuprates) or multiorbital occupancy occurs (as for Fe pnictides).

Alkali doped fullerenes A<sub>3</sub>C<sub>60</sub> (A is alkali ion) represent a distinct family of high transition temperature ( $T_c$ ) SC in a multiorbital case, as the lowest unoccupied C<sub>60</sub> molecular orbitals (named  $t_{1u}$ ) are sixfold degenerate [1]. The importance of electron correlations in A<sub>n</sub>C<sub>60</sub> compounds has been suggested first from the detection of insulating states for even  $n$ , contrary to the expected metallicity for any  $1 \leq n \leq 5$  in an independent electron picture. On-ball localization of pairs of electrons is favored by the energy gain due to Jahn-Teller (JT) distortions of the charged C<sub>60</sub> molecules which adds to the Coulomb energy  $U$ . The occurrence of this Mott Jahn-Teller insulator [2], in which Hund's rule is violated, has been confirmed by the observation by NMR of a spin gap due to singlet-triplet excitations, smaller than the optical gap, for both crystal structures of A<sub>4</sub>C<sub>60</sub> [3] and Na<sub>2</sub>C<sub>60</sub> [4]. Furthermore, for  $n = 1$ , in fcc CsC<sub>60</sub>, the observation of charge segregation of singlet electron pairs on a sizable fraction of the C<sub>60</sub> balls at low  $T$  has been an even more direct evidence that electron pairs are favored by JT distortions [5].

For  $n = 3$ , JT distortions were expected to be less effective. So the  $s$ -wave SC evidenced in the fcc A<sub>3</sub>C<sub>60</sub> and the scaling of  $T_c$  with the distance between C<sub>60</sub> balls have been interpreted by most researchers as purely BCS, driven by on-ball phonons, with weak incidence of electronic correlations [1]. The effort to increase  $T_c$  by expanding the C<sub>60</sub> lattice has, however, led to the discovery of various magnetic compounds, such as (NH<sub>3</sub>)<sub>x</sub>K<sub>3</sub>C<sub>60</sub>, which displays a Mott transition to a SC state under pressure [6]. But one was still led to suspect that this behavior could be

attributed to a lifting of the degeneracy of the  $t_{1u}$  levels by the peculiar lattice structure required to expand the C<sub>60</sub> lattice [7]. The most expanded fulleride Cs<sub>3</sub>C<sub>60</sub> had been found to become SC under pressure ( $p$ ), with  $T_c \approx 40$  K [8], but it has only recently been shown that this occurs in a cubic A15 structure [9]. A renewed interest arises then as this phase is antiferromagnetic (AFM) at ambient  $p$ , with  $T_N = 47$  K [10], and undergoes a Mott transition to a metallic state for  $p \sim 4$  kbar. It is then of great interest to find out whether the electronic properties of A15-Cs<sub>3</sub>C<sub>60</sub> are different from those of other fcc-A<sub>3</sub>C<sub>60</sub> phases.

Gainin *et al.* indicated that the low-temperature reaction process [9] used to synthesize A15-Cs<sub>3</sub>C<sub>60</sub> produces mixed phases including fcc Cs<sub>3</sub>C<sub>60</sub> and body centered orthorhombic (bco) Cs<sub>4</sub>C<sub>60</sub>. Using the spectroscopic capabilities of <sup>133</sup>Cs NMR experiments, we sorted out the signals from the two Cs<sub>3</sub>C<sub>60</sub> isomers in such mixed-phase samples. Taking that as an advantage, we report in this Letter the first direct comparison and demonstrate that a Mott transition to SC occurs as well in fcc Cs<sub>3</sub>C<sub>60</sub>. At ambient pressure, we evidence the decrease of spin freezing temperature for the fcc as compared to that of the A15 phase and associate it with the geometrical frustration of the former lattice. The occurrence of a Mott transition is shown to be independent of the crystal structure and of the specific C<sub>60</sub> ball orientational (merohedral) disorder present in fcc Cs<sub>3</sub>C<sub>60</sub>. This confers then a very important place to these phases helping one to understand SC in the vicinity of magnetic phases.

<sup>133</sup>Cs NMR spectra of the two phases.—We synthesized mixed-phase samples and selected three of them with significantly differing phase contents, labeled A1 and A2 for A15 rich and F1 for the fcc rich. Their compositions are A1 (58.4, 12, 29.5), A2 (41.7, 12, 46.5), F1 (34, 55, 11), where the percent contents in formula units are given, respectively, for the A15, fcc, and bco phases. As <sup>133</sup>Cs has a nuclear spin  $I = 7/2$ , its NMR spectrum is sensitive to the local site symmetry through the coupling of the nuclear quadrupole moment with the electric field gradient (EFG) induced by the local charge distribution. Therefore,

in the A15 phase the single NMR site displays a quadrupole-split seven-line spectrum [Fig. 1(a)], as the unique Cs site displays a noncubic local symmetry [11]. In the fcc phase, the unit cell contains two alkali sites, with occupancy ratio 1:2 for the octahedral ( $O$ ) and tetrahedral ( $T$ ) sites. Their local symmetry being cubic, the EFG vanishes and each site has a narrow nonsplit signal. A peculiarity evidenced by NMR [12] in all formerly known fcc  $A_3C_{60}$  is that the tetrahedral site splits into two sites ( $T$  and  $T'$ ), which have been assigned to the merohedral disorder of  $C_{60}$  balls [13]. The detection in sample F1 of these three lines [Fig. 1(b)] establishes then the identical structure of fcc  $Cs_3C_{60}$ . This difference in NMR spectra allowed us, as was done in Fig. 1, to detect selectively the  $^{133}\text{Cs}$  NMR of a given phase using technical procedures recalled in Ref. [14]. Let us point out, as will be discussed later, that the data of Figs. 1(c) and 1(d) demonstrate that these structures are not modified under pressure.

**Paramagnetism at ambient pressure.**—SQUID data on all samples do not display any superconductivity for  $p = 1$  bar, and only exhibit a paramagnetic susceptibility

$$\chi(T) = \chi_{\text{orb}} + \chi_s(T),$$

which includes an orbital term and a  $T$  dependence due to the spin magnetism of unpaired electrons. The data were similar to those attributed to the A15 phase [10]. Comparisons between the two phases are possible from analyses of the  $^{13}\text{C}$  NMR spectra, as the NMR shift also involves orbital and spin components

$$K^\alpha = K_{\text{orb}}^\alpha + K_s^\alpha(T) = K_{\text{orb}}^\alpha + A^\alpha \chi_s(T).$$

Here, the index  $\alpha$  refers to the direction of the applied field  $B$  with respect to local axes on the  $^{13}\text{C}$  site. Indeed, both  $K_{\text{orb}}^\alpha$ , due to the orbital magnetism of the  $sp^2$  bonding electrons [15], and  $K_s^\alpha(T)$ , associated with the spin mag-

netization of electrons in the  $t_{1u}$  orbitals, are anisotropic [16]. The random orientation of the balls with respect to  $B$  gives a typical  $^{13}\text{C}$  powder NMR spectrum, with two singularities for  $K^\perp$  and  $K^\parallel$  which correspond to  $B$  directions  $\perp$  and  $\parallel$  to the tangential plane to the  $C_{60}$  ball at the  $^{13}\text{C}$  site, as shown in the inset of Fig. 2(a). One can notice there that, at  $T = 160$  K, the spectra are identical for the A15 and fcc rich samples.

Furthermore, in Fig. 2(a) the  $T$  variations of the anisotropy  $^{13}K^{\text{ax}} = 2(K^\perp - K^\parallel)/3$ , which is obtained from fits of the spectra, cannot be differentiated for the two phases above 100 K and track those of SQUID data for  $\chi$  taken on sample A1. The deduced data for  $\chi_s(T)$  are then intrinsic and similar for both phases and can be fitted above 100 K with a Curie-Weiss law with an effective moment  $p_{\text{eff}} = 1.52(5)\mu_B$  per  $C_{60}$  and a Weiss temperature  $\Theta_W = -70 \pm 5$  K. Such a value for  $p_{\text{eff}}$  lets us suggest that the  $C_{60}^{3-}$  ion is in a low spin state in the fcc phase as established before for the A15 phase [10,11].

**Magnetic ordering at ambient pressure.**—For all samples the SQUID data exhibit a sharp increase of magnetization at  $T = 47$  K due to the AFM state of the fraction of A15 phase as shown in Fig. 2(a). We also detected the

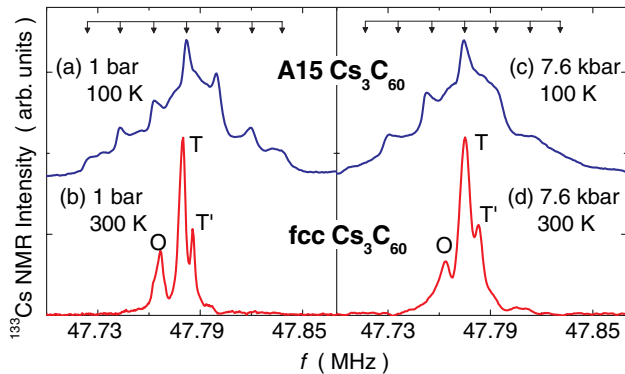


FIG. 1 (color online). (a) The A15  $^{133}\text{Cs}$  NMR spectrum taken at ambient pressure displays a seven-peak powder NMR spectrum (arrows), with a quadrupole splitting of  $\sim 39$  kHz at 100 K, and a slight asymmetric spectral shape originating from a Knight shift anisotropy. (b)  $^{133}\text{Cs}$  NMR spectra for the fcc phase displaying the octahedral  $O$  and tetrahedral  $T$  and  $T'$  site peaks. (c), (d) The spectra are found nearly unmodified at 7.6 kbar when both phases are metallic (see text).

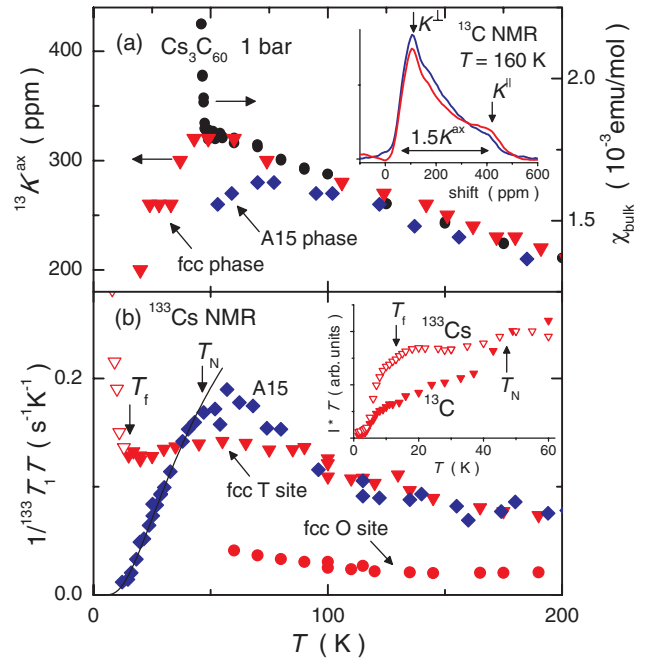


FIG. 2 (color online). Ambient pressure data taken in samples A1 and F1 for the A15 and fcc phases. (a) Similar variations above 100 K of the anisotropic shift contribution  $^{13}K^{\text{ax}}$  to the  $^{13}\text{C}$  spectra (displayed in the inset). The scale chosen on the right for  $\chi$  (black dots, SQUID data on A1) emphasizes the linear relation with  $^{13}K^{\text{ax}}$ . (b)  $^{133}\text{Cs}$   $(T_1T)^{-1}$  data for the fcc phase  $T$  site and the A15 phase have similar high  $T$  variations but differ markedly near and below their ordered magnetic states. The spin freezing at  $T_f$  in the fcc phase is monitored in the inset at the onset of decrease of the  $^{13}\text{C}$  signal intensity (see text). Open symbols are  $(T_1T)^{-1}$  data for  $T$ .

increased linewidth of the A15 phase  $^{133}\text{Cs}$  NMR signal found in Refs. [10,11]. We could as well find in the A15 rich sample that the magnetization on the  $\text{C}_{60}$  ball induces such a large broadening of the  $^{13}\text{C}$  NMR that its intensity, detected within a small frequency window of 100 kHz (that is 0.01 T), vanishes below  $T_N = 47$  K. This allowed us then in sample *F1*, after the loss of the A15 fraction ( $\sim 40\%$ ), to isolate below 47 K the fcc  $^{13}\text{C}$  NMR. The paramagnetism of this phase, given by  $^{13}K^{\text{ax}}$ , decreases slightly with respect to its high  $T$  value, as seen in Fig. 2(a).

Spin freezing in the fcc is only detected below  $T_f \approx 10$  K from the sharp intensity drops of both the  $^{13}\text{C}$  and the fcc-specific  $^{133}\text{Cs}$  NMR signal, shown in the inset of Fig. 2(b). This latter observation establishes that in the fcc-frozen spin state the internal field on the  $^{133}\text{Cs}$  sites is then much larger than that in the A15 AFM phase for which the integrated intensity over a 100 kHz window only slightly declines below  $T_N$ . This, together with the small  $T_f$  value, is evidence that the fcc magnetic state is influenced by the inherent frustration of this lattice, contrary to the A15 phase AFM phase, for which the transferred internal field on  $^{133}\text{Cs}$  is partly compensated due to the bipartite body centered lattice symmetry[11]. On the contrary, this large internal field on  $^{133}\text{Cs}$  and the small  $T_f$  value give evidence that the fcc phase magnetic state is influenced by the inherent frustration of the fcc lattice.

To compare the dynamical magnetic properties,  $^{133}\text{Cs}$  spin lattice relaxation  $T_1$  data have been taken on the two phases. In the fcc, the less shifted  $O$  site could only be resolved above 50 K, and its  $T_1$  scales by a factor of 3 with that of the  $T$  site, as seen in Fig. 2(b). Thus both sites sense the same magnetic fluctuations through distinct hyperfine couplings. For the  $T$  site,  $(T_1 T)^{-1}$  follows in the paramagnetic regime a similar variation as that seen in the A15 phase. There, below  $T_N = 47$  K a sharp gap in the spin excitations is detected and the data can be fitted with  $(T_1 T)^{-1} \propto \exp(-\Delta/k_B T)$ , with  $\Delta/k_B \approx 50$  K [full line in Fig. 2(b)]. On the contrary, in the fcc phase  $(T_1 T)^{-1}$  remains nearly constant down to 10 K and even displays a fast increase for the  $^{133}\text{Cs}$  sites which are not submitted to a large static field. This persistence of spin fluctuations at low  $T$  is also to be linked to frustration effects.

*SC phases under pressure and phase diagram.*—SC diamagnetism could be probed *in situ* by monitoring the shift of the NMR coil tuning frequency ( $f \approx 28$  MHz). This allowed us to estimate the SC volume fractions, as we kept the geometry unchanged during the pressure sweeps. We find here that the fcc phase displays a transition to a SC state at 3.9 kbar (sample *F1*), while this occurs only above 5.5 kbar in the A15 rich (*A2*), which points out that the critical pressure  $p_c$  for the magnetic-SC transition is lower for the fcc phase than for the A15. This can be seen in the inset of Fig. 3, where the magnitude of the diamagnetic signal measured at 10 K is plotted versus  $p$ . It is as well compared for the A15 phase with the magnetic volume fraction estimated from the  $^{133}\text{Cs}$  NMR as described in

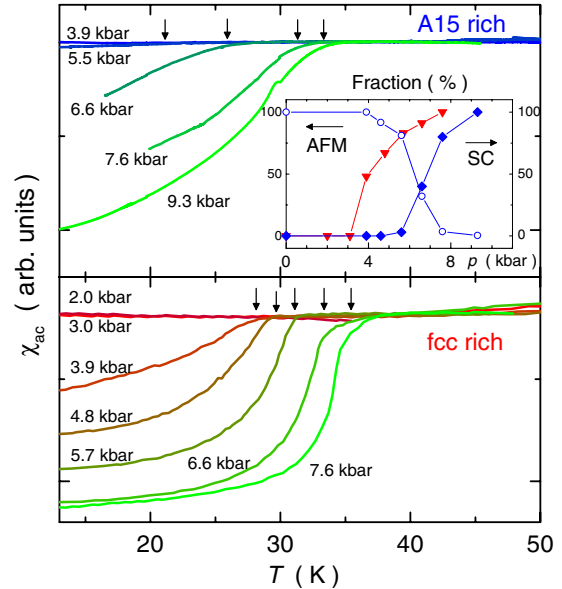


FIG. 3 (color online). SC diamagnetism is detected at a lower  $p_c$  for the sample *F1* than for *A2* (nearly pure A15). The arrows point out the values of  $T_c(p)$  deduced by extrapolation of the sharp  $T$  dependent diamagnetism (slightly smaller than the onset). The diamagnetic magnetization at 10 K (extrapolated for some  $p$  values) is displayed in the inset for both samples, together with the AFM volume fraction for the A15 phase (see [14]).

[14]. The abrupt loss of magnetism above 7 kbar and onset of SC above 6 kbar points to the first-order AFM/SC phase boundaries at  $p_c = 6.5(5)$  kbar in the A15 and  $p_c = 3.5(5)$  kbar in the fcc phase.

We can then report the  $(p, T)$  phase diagrams in Fig. 4(a), and find in Fig. 4(b) that  $p_c$  and  $T_c$  merge together for the two  $\text{Cs}_3\text{C}_{60}$  phases if plotted versus  $V_{\text{C}_{60}}$ , the unit volume per  $\text{C}_{60}$  ball [17]. There, we can as well compare the present  $T_c$  data with former results on the other fcc  $\text{A}_3\text{C}_{60}$ , and we evidence that a similar maximum of  $T_c$  versus  $V_{\text{C}_{60}}$  applies for the two structures.

Let us now consider the NMR data taken at high enough  $p$ , for which both phases become SC at low  $T$ . It is first clear, as seen in Fig. 1, that the spectra above  $T_c$  do not differ from those taken at 1 bar. This absence of structural modification for both phases establishes then that the evolution with  $p$  only implies electronic degrees of freedom.

In the metallic state, a Korringa-like  $T$  independent  $T_1 T$  is seen above  $T_c$  for the two phases as shown in Fig. 5. The constant values are similar for  $^{133}\text{Cs}$  in the A15 as for the  $T$  site of the fcc, which displayed similar  $T_1$  in the paramagnetic phases as well [Fig. 2(b)]. This points out that the spin dynamics has comparable evolution with pressure in the two phases. In the A15, the opening of the SC gap at  $T_c$ , as detected from the onset of decrease in the  $^{133}\text{Cs}$  Knight shift  $^{133}K$ , occurs slightly above the observed decrease in  $(T_1 T)^{-1}$  for both  $^{13}\text{C}$  and  $^{133}\text{Cs}$  nuclei. This result perfectly mimics the observations done in high applied fields in the other fcc- $\text{A}_3\text{C}_{60}$  compounds [18]. There, such a persistence

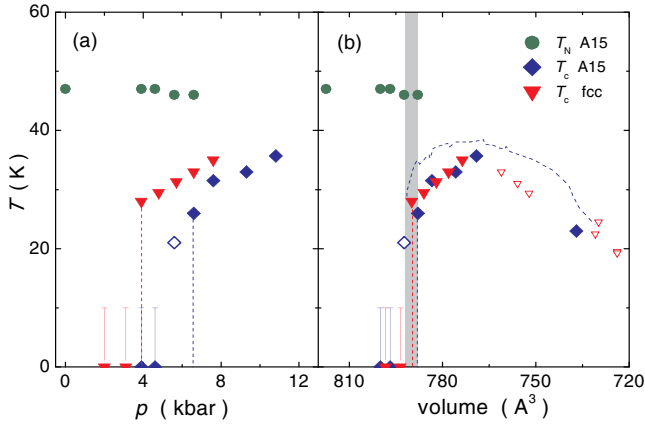


FIG. 4 (color online). Phase diagram reporting the critical temperatures (a) versus  $p$  and (b) versus  $V_{C_{60}}$ . The pressures  $p_c$  of the Mott transitions shown as dotted lines in (a) merge into the gray area in (b). There we reported for comparison the former data on A15 phase [10] as a dotted line, and on the other fcc  $A_3C_{60}$  as open downward triangles [21].

of spin excitations slightly below  $T_c$  are remnants of the  $s$ -wave BCS-like Hebel-Slichter coherence peak [19], which is damped in high fields and could only be fully revealed from low field data [1].

**Summary and discussion.**—In conclusion, we have shown here that the magnetic ground states of the  $Cs_3C_{60}$  phases are quite distinct at ambient pressure. The reduction of ordering temperature and the persistence of low-energy spin fluctuations at low  $T$  in the fcc phase can be assigned to the frustration effects inherent to this structure and its merohedral disorder. We further evidenced that no major crystal structure modification occurs under pressure as shown as well from x-ray diffractograms in the A15 phase [10]. Thus the low  $T$  transition from a magnetic to a SC state, which appears to be of first order, is fully determined by electronic parameters in both cases. Comparison of the phase diagrams demonstrates that the critical pressure  $p_c$  for the transition occurs for a similar value of the volume

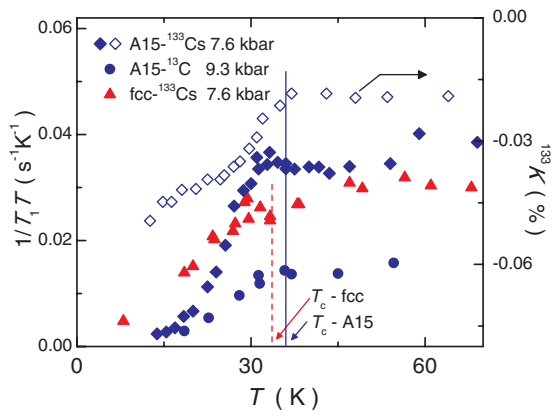


FIG. 5 (color online).  $T$  variation above  $p_c$  of  $(T_1T)^{-1}$  for  $^{133}\text{Cs}$  and  $^{13}\text{C}$  (filled symbols) and the  $^{133}\text{Cs}$  shift  $K$  (open diamonds) in the A15 phase. The full and dotted lines point out the  $T_c$  values in the applied field for the two phases.

per  $C_{60}$  ball  $V_{C_{60}}$ , which highlights the Mottness of the transition to be opposed to a charge or spin density wave transition, which should sensitively depend on lattice and Fermi surface symmetry.

Our data evidence that fcc- $A_3C_{60}$  compounds exhibit a dome behavior of  $T_c(V_{C_{60}})$ , identical to that found in the A15 phase under pressure. This unexpected feature in a purely BCS  $s$ -wave scenario dominated by a density of state variation is then quite generic. Our result then gives weight to the theoretical attempts to take correlation and JT effects into account in these systems [20], which did suggest such a behavior beforehand. We are presently investigating the evolution of the spin dynamics across the Mott transition, which should permit more thorough comparisons with such theoretical approaches, and hope that the present work will trigger diverse other experimental studies of the electronic properties of the  $Cs_3C_{60}$  phases across the Mott transition.

We thank V. Brouet, M. Fabrizio, and E. Tosatti for their interest and for stimulating exchanges. Y. I acknowledges financial support from JSPS for his stay in Orsay.

\*ihara@lps.u-psud.fr

- [1] O. Gunnarsson, *Rev. Mod. Phys.* **69**, 575 (1997).
- [2] M. Capone, M. Fabrizio, P. Giannozzi, and E. Tosatti, *Phys. Rev. B* **62**, 7619 (2000).
- [3] R. Kerkoud *et al.*, *J. Phys. Chem. Solids* **57**, 143 (1996).
- [4] V. Brouet, H. Alloul, S. Garaj, and L. Forró, *Phys. Rev. B* **66**, 155122 (2002).
- [5] V. Brouet, H. Alloul, F. Quéré, G. Baumgartner, and L. Forró, *Phys. Rev. Lett.* **82**, 2131 (1999).
- [6] K. Prassides *et al.*, *J. Am. Chem. Soc.* **121**, 11 227 (1999).
- [7] M. J. Rosseinsky, D. W. Murphy, R. M. Fleming, and O. Zhou, *Nature (London)* **364**, 425 (1993).
- [8] T. T. M. Palstra *et al.*, *Solid State Commun.* **93**, 327 (1995).
- [9] A. Y. Ganin *et al.*, *Nature Mater.* **7**, 367 (2008).
- [10] Y. Takabayashi *et al.*, *Science* **323**, 1585 (2009).
- [11] P. Jeglič *et al.*, *Phys. Rev. B* **80**, 195424 (2009).
- [12] R. E. Walstedt, D. W. Murphy, and M. Rosseinsky, *Nature (London)* **362**, 611 (1993).
- [13] P. Matus, H. Alloul, G. Kriza, V. Brouet, P. M. Singer, S. Garaj, and L. Forro, *Phys. Rev. B* **74**, 214509 (2006).
- [14] See supplementary material at <http://link.aps.org/supplemental/10.1103/PhysRevLett.104.256402> for the technical NMR procedures used to select the signals.
- [15] R. Tycko *et al.*, *Phys. Rev. Lett.* **67**, 1886 (1991).
- [16] C. H. Pennington and V. A. Stenger, *Rev. Mod. Phys.* **68**, 855 (1996).
- [17] The unit cell volume per  $C_{60}$ ,  $V_{C_{60}}$ , was estimated using the compressibilities of 5.4 and 5.9 ( $10^{-3}$  kbar $^{-1}$ ) for the fcc and A15 phases, respectively [10].
- [18] V. A. Stenger, C. H. Pennington, D. R. Buffinger, and R. P. Ziebarth, *Phys. Rev. Lett.* **74**, 1649 (1995).
- [19] L. C. Hebel and C. P. Slichter, *Phys. Rev.* **113**, 1504 (1959).
- [20] M. Capone, M. Fabrizio, C. Castellani, and E. Tosatti, *Science* **296**, 2364 (2002).
- [21] Y. Maniwa *et al.*, *J. Phys. Soc. Jpn.* **63**, 1139 (1994).